SUPPLEMENTARY FIGURES

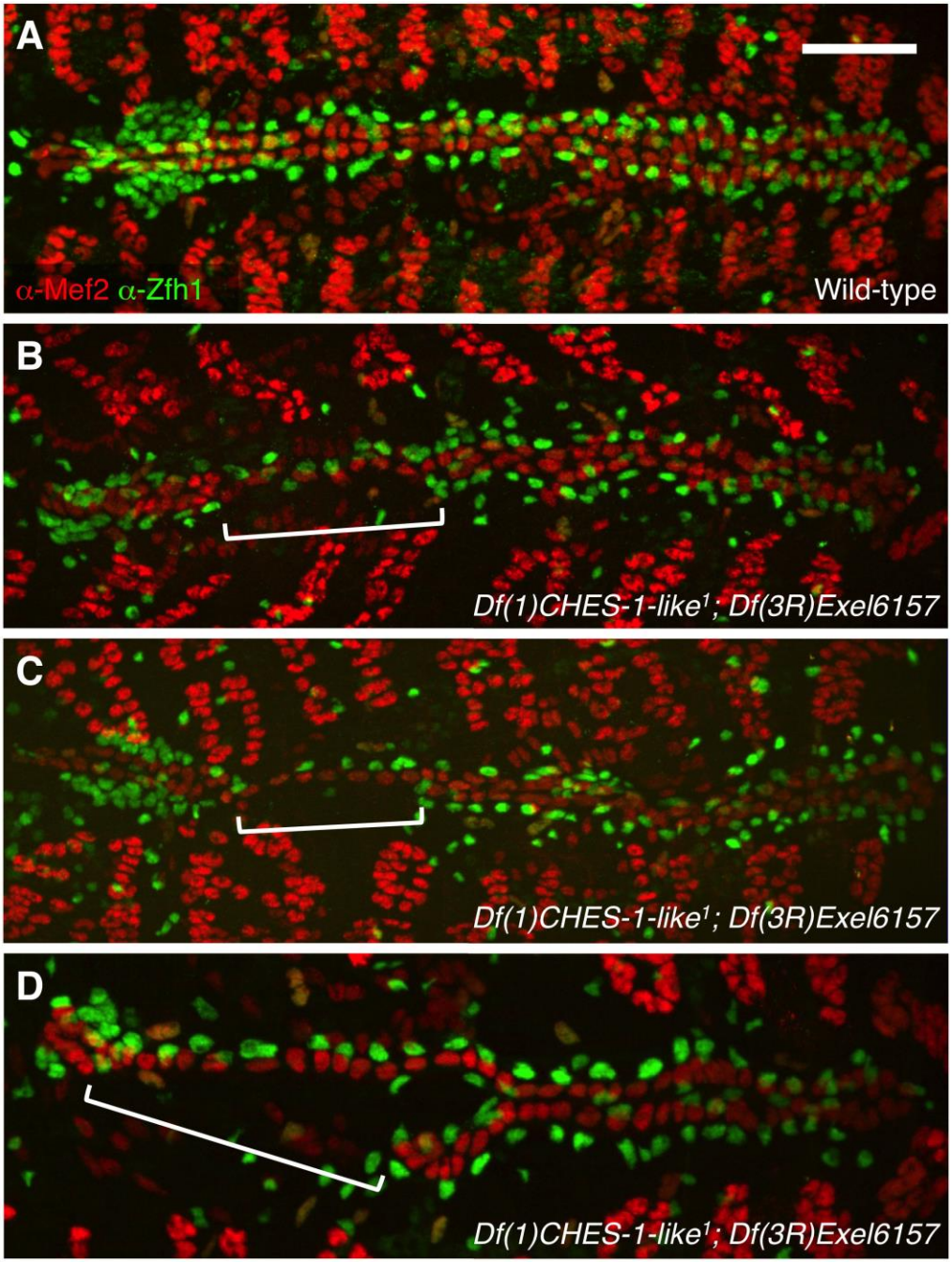

Fig. S1. Missing cardiac hemisegments (MCH) phenotypes associated with embryos lacking both *CHES-1-like* and *jumu* functions. (A-D) Mef2 antibody staining (red) of cardial cells (CCs) and Zfh1 antibody staining (green) of pericardial cells (PCs),

illustrating the presence or absence of the MCH phenotype (square brackets), in representative Stage 16 embryos that are (A) wild-type and (B-D) doubly homozygous for both a *CHES-1-like* null mutation and a *jumu* null deficiency. Note that each hemisegment in the wild-type embryo (A) consists of a row of CCs associated with multiple PCs. Hemisegments lacking CCs in the *CHES-1-like; jumu* double homozygotes (B-D) are also missing PCs. Scale bar: 50 μm.

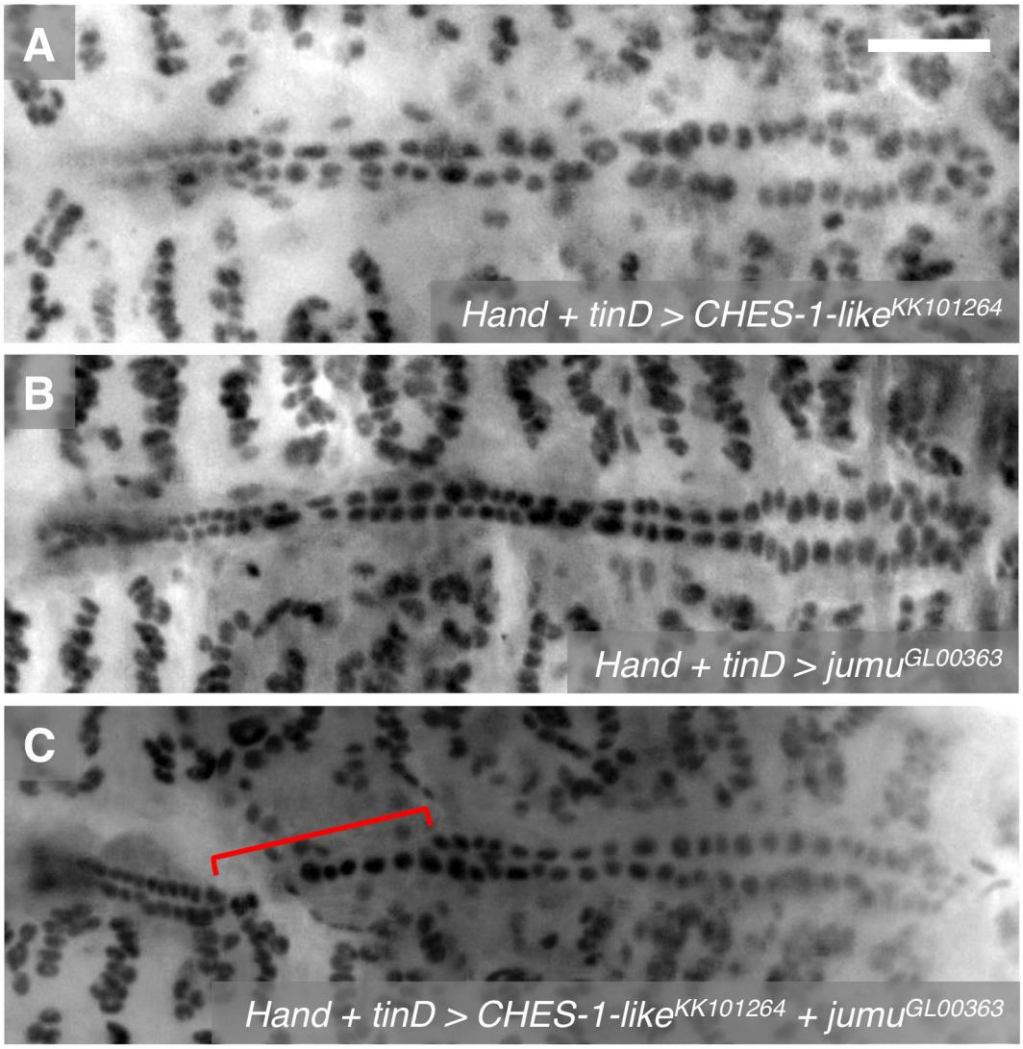

Fig. S2. Missing cardiac hemisegments (MCH) phenotypes are detected when both *CHES-1-like* and *jumu* functions are simultaneously disrupted specifically in cardiac mesoderm precursors. (A-C) Mef2 antibody staining of CCs illustrating the presence or absence of the MCH phenotype (square brackets) in representative Stage 16 embryos in which (A) *CHES-1-like* function, (B) *jumu* function, or (C) both *CHES-1-like* and *jumu* functions simultaneously have been knocked down by CM precursor-targeted RNA interference directed by the *tinD-GAL4* and *Hand-GAL4* drivers. Scale bar: 50 μm.

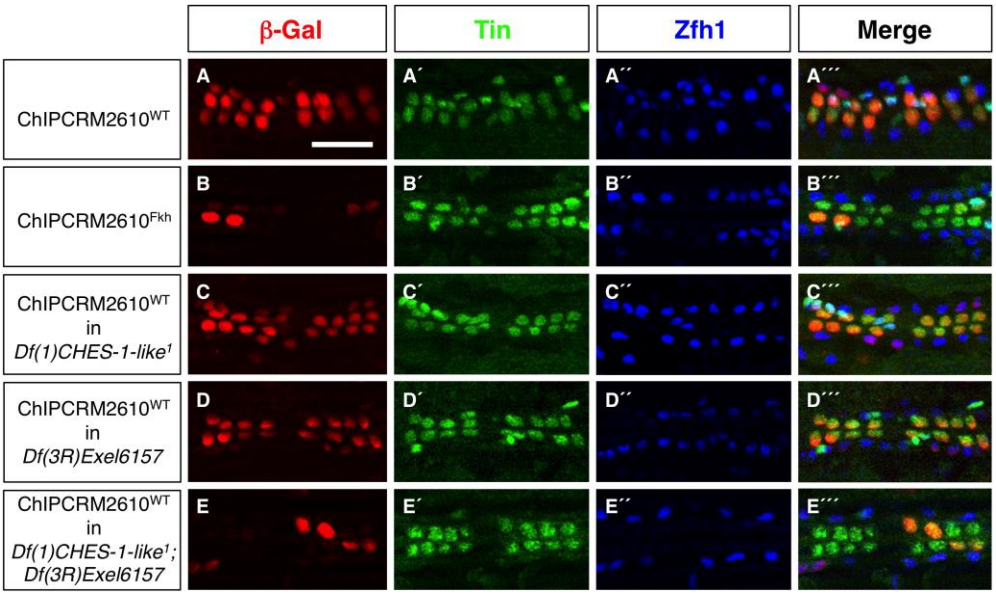

Fig. S3. CHES-1-like and Jumu act in a mutually redundant manner to activate expression from the enhancer. The posterior-most four CCs in a hemisegment are marked by Tin expression (green), while the PCs are marked by Zfh1 expression (blue) (**A**) β-galatosidase reporter (red) driven by the wild-type *htl* enhancer (ChIPCRM2610^{WT}) is expressed primarily in the four Tin-expressing CCs. (B) Mutating the Fkh binding site in the enhancer (ChIPCRM2610^{Fkh}) results in significant reduction of reporter activity in the Tin-CCs. (C) Reporter activity driven by the wild-type enhancer (ChIPCRM2610^{WT}) is not significantly affected in embryos lacking *CHES-1-like* function. (D) Reporter activity driven the wild-type enhancer is also not significantly affected in embryos lacking *jumu* function. (E) In contrast, embryos lacking both *CHES-1-like* and *jumu* functions exhibit significantly reduced reporter activity from the wild-type enhancer (A), comparable to that of the enhancer with the mutated Fkh binding site (B). Scale bar: 25 μm.

Table S1. Comparison of the Missing Cardiac Hemisegments (MCH) phenotypes in anterior and posterior hemisegments in embryos lacking both *CHES-1-like* and *jumu* functions.

Click here to Download Table S1

Table S2. Genes exhibiting differential expression due to perturbations in the functions of *CHES-1-like*, *jumu*, *htl* and *wg*. (A) Genes activated by CHES-1-like: genes corresponding to probesets exhibiting $\log_2$ Fold Change < 0 and adjusted *p*-value < 0.1 in purified mesodermal cells homozygous for the *CHES-1-like* null mutation. Known cardiac genes (Ahmad et al., 2012) and genes downregulated in purified mesodermal cells homozygous for *wg* null mutations (Table S2E) are identified. (B) Genes repressed by *CHES-1-like*: genes corresponding to probesets exhibiting $\log_2$ Fold Change > 0 and adjusted *p*-value < 0.1 in purified mesodermal cells homozygous for the *CHES-1-like* null mutation. Known cardiac genes are identified. (C) Genes activated by Jumu: genes corresponding to probesets exhibiting $\log_2$ Fold Change < 0 and adjusted *p*-value < 0.1 in purified mesodermal cells homozygous for the *jumu* null deficiency. Known cardiac genes and genes downregulated in purified mesodermal cells homozygous for a *wg* null mutation (Table S2E) are identified. (D) Genes repressed by Jumu: genes corresponding to probesets exhibiting $\log_2$ Fold Change > 0 and adjusted *p*-value < 0.1 in purified

mesodermal cells homozygous for the *jumu* null deficiency. Known cardiac genes are identified. (E) Genes activated by Wg: genes corresponding to probesets exhibiting $\log_2$ Fold Change < 0 and adjusted *p*-value < 0.1 in purified mesodermal cells homozygous for *wg* null mutations. Genes downregulated in purified mesodermal cells homozygous for the *CHES-1-like* null mutation (Table S2A) or for the *jumu* null deficiency (Table S2C) are identified. (F) Genes corresponding to probesets exhibiting $\log_2$ Fold Change > 0 and adjusted *p*-value < 0.1 in purified mesodermal cells as a consequence of ectopic mesodermal overexpression of Jumu. Genes upregulated in purified mesodermal cells due to the ectopic mesodermal overexpression of a constitutively activated form of Htl (Table S2G) are identified. (G) Genes corresponding to probesets exhibiting $\log_2$ Fold Change > 0 and adjusted *p*-value < 0.1 in purified mesodermal cells as a consequence of ectopic mesodermal overexpression of a constitutively activated form of Htl. Genes upregulated in purified mesodermal cells due to the ectopic mesodermal overexpression of Jumu (Table S2F) are identified. Genesets used for Fisher tests were comprised only of genes where all probesets for a particular gene exhibited significant differential expression in the same direction for a particular perturbation.

Click here to Download Table S2

SUPPLEMENTARY MATERIALS AND METHODS

Statistical Analyses

To determine if missing cardiac hemisegments occurred preferentially in the anterior or posterior positions, we examined how likely it is to observe differences in anterior and posterior MCH errors as extreme as (or more extreme than) what was observed. The analysis was performed conditional on the number of MCH errors (either anterior or posterior) that was observed. As shown in Supplementary Table S1, of the 128 embryos, 22 showed MCH in either anterior or posterior positions. Of these 22 occurrences, 12 were anterior and 10 were posterior. Under the null hypothesis that errors are equally likely to occur in either position, the probability of observing results as extreme as this 12/10 split is 0.83. This p-value of 0.83 indicates there is no strong evidence to conclude MCH occurs preferentially in either the anterior or posterior position.

Fisher's exact test was used for comparisons of MCH phenotype rates by genotype in Table 1 and Figs. 1, 5, 7 and 8.

Bootstrap and permutation methods were used for the analyses in Fig. 4 and Table 2 that compared reporter expression among enhancer-genotype groups. This approach was used instead of Fisher's exact test or other methods because the unit of analysis is a hemisegment within an embryo and results from different hemisegments within an embryo are not statistically independent.

In Fig. 4F confidence intervals for the mean number of Tin-CCs exhibiting reporter activity per hemisegment were computed using bootstrap methods (Davison and Hinkley, 1997). Specifically, for a given genotype, the embryos were sampled with replacement to construct a sample of the original size and the mean number of Tin-CCs with activity per

hemisegment was calculated. This process was repeated 10,000 times and an empirical distribution of mean values was obtained. The 95% confidence interval is given by ($mean_{0.025}$, $mean_{0.975}$) where $mean_{0.025}$ designates the 250^{th} smallest of the 10,000 empirical means and $mean_{0.975}$ designates the 9750^{th} smallest of the means. Such an approach takes into account the within-embryo correlation among hemisegments and produces confidence intervals that cannot exceed 4 nor be less than 0 (this is not the case for intervals constructed using some formulas for standard error).

Also in Fig. 4F, permutation testing was used to obtain p-values for testing the hypothesis that the mean number of Tin-CCs with reporter activity per hemisegment was equivalent in two genotypes. Given two genotypes, one first computed the average number of Tin-CCs with activity per hemisegment in each group and the difference in means between the two genotypes was recorded. Next, 10,000 simulated datasets were created in which the mutation group assignments were randomly permutated (i.e. exchanged) between the embryos in the two groups. For each simulated dataset the difference in the average number of Tin-CCs with activity per hemisegment was calculated as before, though now using the randomly assigned mutation group designations. The 10,000 datasets produce 10,000 differences that would be equally likely to be obtained under the null hypothesis that there is no difference in enhancer expression between the mutation groups. The permutation p-value is obtained by determining the proportion of the 10,000 differences that, in absolute value, were greater than or equal to the initial difference obtained using the original data (Good, 1994). Similar bootstrap and permutation methods were used for Fig. 4G.

In Figs. 1 and 6, a bootstrap approach was used to obtain p-values for determining whether non-additive interactions exist among mutation types. The tests are based on 10,000 bootstrap samples. A bootstrap sample was drawn from the genotype with both mutations and the proportion of errors for the genotype was calculated. This average was subtracted from the sum of averages obtained from bootstrap samples of each of the two genotypes with one mutation. From this subtraction a single estimate of the interaction was obtained. The procedure was then repeated 10,000 times: each time corresponded to computing average error counts for the three genotypes and thus obtaining 10,000 estimates of the interaction. P-values for the hypothesis of no interaction were obtained by examination of the proportion of bootstrapped interactions above and below 0.

Geneset Enrichment

Probeset-level microarray data for *Df(1)CHES-1-like*[1] and *Df(3R)Exel6157* (as compared to wild-type) were annotated for associated genes with the Drosophila_2.na34.annot.csv file from Affymetrix using the "Gene Symbol" field. Probesets with associated gene symbols found in the list of heart-expressed genes assembled in Ahmad et al. (2012) were annotated as "heart" probesets; all probesets were ranked by the absolute value of the *limma* t statistic, and enrichment of heart probesets among high-ranking (differentially regulated) probesets was assessed with the wilcox.test function in R.

To compare enriched/depleted genesets among conditions, probeset-level microarray data for Htl gain of function and *wg* loss of function (as compared to wild type) from Estrada et al. (2006) were annotated as above with the DrosGenome1.na21.annot.csv file from Affymetrix. Significantly enriched or depleted probesets were defined by a *limma*

adj.P.Val (adjusted P value) < 0.1; a gene was considered part of an enriched or depleted geneset for this analysis if all probesets associated with it were significantly enriched or depleted (respectively) and its annotation was present in common in both microarray designs. The overlap between two genesets was counted with the venn function in the R gplots package, and significance of enrichment or depletion was assessed with the fisher.test function.

SUPPLEMENTARY REFERENCES

Ahmad, S. M., Tansey, T. R., Busser, B. W., Nolte, M. T., Jeffries, N., Gisselbrecht, S. S., Rusan, N. M. and Michelson, A. M. (2012). Two forkhead transcription factors regulate the division of cardiac progenitor cells by a Polo-dependent pathway. *Dev Cell* **23**, 97-111.

Davison, A. C. and Hinkley, D. V. (1997). *Bootstrap Methods and Their Application*. Cambridge: Cambridge University Press.

Good, P. I. (1994). *Permutation Tests: A Practical Guide to Resampling Methods for Testing Hypotheses*. New York: Springer-Verlag.